

Tunneling anisotropic magnetoresistance in organic spin valves

M. Grünewald^{1,2}, M. Wahler^{1,2}, M. Michelfeit^{1,2}, C. Gould^{1,2}, R. Schmidt^{2,3}, P. Graziosi⁴, A. Dediu⁴, F. Würthner^{2,3}, G. Schmidt^{1,2,5}, and L.W. Molenkamp^{1,2}

¹*Physikalisches Institut (EP3)*, ²*Röntgen Center for Complex Material Systems*,

³*Institut für Organische Chemie, Universität Würzburg*,

Am Hubland, 97074 Würzburg, Germany

⁴*Institute of Nanostructured Materials*,

ISMN-CNR, via Gobetti 101, 40129 Bologna, Italy

⁵*Institut für Physik, Martin-Luther-Universität Halle-Wittenberg, D-06099, Germany**

**present and permanent address G.S.*

Correspondence to G. Schmidt email: georg.schmidt@physik.uni-halle.de

Abstract

We report the observation of tunneling anisotropic magnetoresistance (TAMR) in an organic spin valve with only one ferromagnetic electrode. The spin valve is based on a new high mobility perylene diimide-based n-type organic semiconductor. We attribute the TAMR to tunneling injection processes from the epitaxial Lanthanum Strontium Manganite electrode which dominates the transport properties. The typical switching pattern originates from the magnetocrystalline anisotropy of the epitaxial magnetic electrode.

Over the past years a number of spin valves based on various organic semiconductors and contact materials have been demonstrated[1, 2, 3, 4, 5, 6]. While for many experiments it is still unclear whether they show tunneling magnetoresistance or actual spin injection and consequently giant magnetoresistance, all signals are interpreted to be related to the switching of two magnetic electrodes between parallel and antiparallel magnetization configuration and back. We have fabricated a number of different spin-valve like structures (Fig. 1a) using the organic semiconductor (OSC) N,N' -bis(*n*-heptafluorobutyl)-3,4:9,10-perylene tetracarboxylic diimide (PTCDI-C4F7, Fig. 1b). While most spin-valves reported up to now are either based on ALQ₃[2], which is an amorphous low mobility n-type semiconductor, or on p-type semiconductors such as P3HT[3] or TPP[4], PTCDI-C4F7 is a new air-stable, high-mobility n-type semiconductor[7] from the perylene diimide/dianhydride family whose most common member is PTCDI. Owing to its favorable electron transport properties, PTCDI-C4F7 should be well-suited for the demonstration of spin-polarized electron transport. Three different device types were investigated, distinguished by the combinations of contact materials as listed in table I.

<i>device</i>	<i>bottom contact</i>	<i>PTCDI-C4F7 layer</i>	<i>top contact</i>
1	15 nm LSMO	100 nm	30 nm CoFe
2	10 nm Al	250 nm	30 nm Al
3	10 nm LSMO	150 nm	15 nm Al

TABLE I: Contact materials and layer thicknesses of the three investigated multilayers.

Type-1 devices which have an LSMO bottom- and a ferromagnetic metal top-contact are similar to those reported for most organic spin valves (OSVs) in the literature and serve to demonstrate the suitability of PTCDI-C4F7 for spin valve operation. Type-2 devices are control samples with only non-magnetic electrodes and help to exclude possible artifacts caused by the OSC. Type-3 devices have one magnetic LSMO electrode and a non-magnetic Al counter electrode. These samples are intended for investigations on the occurrence of tunneling anisotropic magnetoresistance (TAMR). All layer stacks are deposited in a UHV chamber designed to allow for the deposition of OSC and metal layers in direct sequence without breaking the UHV.

The LSMO bottom contacts are fabricated from 10 or 15 nm thick LSMO layers, grown by pulsed plasma deposition on Strontium Titanate substrates. For device fabrication, first a Ti/Au metal stripe is deposited on the LSMO, using optical lithography and lift-off. This serves as an alignment mark and later as a bondpad. A rectangular bottom contact is then patterned into the LSMO layer by optical lithography and dry etching, leaving the metal contact at one side of the rectangle. Subsequently, the sample is inserted into the UHV-deposition chamber where a bake-out procedure is performed at 450 °C for 1 hour at an oxygen pressure of 10^{-5} mbar, in order to compensate under-oxygenation which may occur during the processing. Subsequently, the PTCDI-C4F7 layer and the metal top electrode are deposited under different angles of incidence through a shadow mask with a rectangular opening. After removing the sample from the UHV chamber, Ti/Au stripes are deposited through a second shadow mask with striped windows. These metal stripes are later used as bond pads for the top contacts and also serve as an etch mask for the removal by dry etching of the top electrode material between the stripes. Samples with aluminum bottom electrode are fabricated on a Si substrate with a 200 nm thick thermal SiO₂ cover layer. A Ti/Au contact pad is deposited before inserting the sample into the UHV chamber where the bottom aluminum layer, the PTCDI-C4F7 layer and the top aluminum layer are evaporated through the shadow mask at three different angles of incidence. The different angles are necessary in order to allow for insulation between top and bottom electrode. After removing the sample from the UHV chamber the processing continues in the same way as for the LSMO based samples. This approach provides clean, oxygen-free, and reproducible interfaces. The samples are characterized at various temperatures between 4.2 K and room temperature, either in a flow cryostat with an external room temperature electromagnet (600 mT) or in a ⁴He bath cryostat with a vector field magnet in which magnetic fields up to 300 mT can be applied in any direction.

A typical magnetoresistance trace of an LSMO/OSC/CoFe spin valve at 4.2 K is shown in fig. 2. The magnetoresistance has at least two distinct components. The first comprises the two sharp switching events for each of the scan directions, which are usually attributed to spin valve operation. For our Type-1 layer stacks (one LSMO and one CoFe metal electrode), this effect is always negative and varies between 1% and 30 % from device to device. The other component is a continuous increase of the resistance with increasing magnetic field corresponding to an effect named organic magnetoresistance (OMAR) which has also been

observed in many organic spin-valves[14].

The type-2 layer stack, which has no magnetic electrodes, is intended for magnetoresistance measurements on the pure OSC. The devices exhibit no detectable magnetoresistance, neither spin-valve nor OMAR(Fig.3). We can thus exclude OSC-related magnetoresistance effects as explanation for the effects found in samples with magnetic contact layers.

The 3rd type of layer stack, with a ferromagnetic LSMO bottom contact and a non-magnetic aluminum counter electrode, has an OSC layer thickness of 150 nm. For such a device, with two metallic Schottky contacts to an OSC layer, the I/V characteristics are typically dominated by charge injection processes at the contacts[15]. The I/V characteristics we observe (Fig. 4) are strongly reminiscent of tunneling processes, which may either be caused by the tunneling injection characteristics of the contacts or by a tunneling process through the OSC layer itself. The relatively weak temperature dependence (increase in resistance by one order of magnitude between room temperature and 4.2 K) suggests that what we observe is pure tunneling, but the relatively low resistance implies tunneling through a thin OSC layer. The evaporation of the top layer likely leads to intermixing and a reduction of the effective OSC thickness[2, 3].

Because there is only one magnetic layer present in type-3 stacks, no genuine spin valve signal can be expected. Nevertheless, the magnetoresistance scans show the two-state behaviour characteristic of a spin-valve. The magnetoresistance curves taken at a bias voltage of 255 mV (fig. 5) clearly exhibit two spin-valve like switching events superimposed to the OMAR. The OMAR effect, although still not fully understood in detail, has been widely observed in OSCs even in fully non-magnetic layer stacks[14]. The spin-valve-like signal, however, must have a different origin than in typical OSV stacks because both TMR and GMR require two ferromagnetic electrodes.

We interpret these data as TAMR. This recently discovered effect allows for spin-valve functionality in layer stacks with only one ferromagnetic contact. At the same time, because of the similar phenomenology, TAMR often complicates the interpretation of spin-valve-like signals in magnetoresistance experiments. The effect was first observed in (Ga,Mn)As [8] and has since been reported to occur in various tunnel contacts on ferromagnetic semiconductors and metals[9, 10, 11, 12]. TAMR is due to a variation of the tunneling probability with magnetization direction caused by magnetocrystalline anisotropy of the magnetic material. For electrodes with biaxial anisotropy the magnetoresistance traces can appear identical to

those observed for a normal spin valve. TAMR in such a system is usually characterized by two distinct remanent resistance states which are selected depending on the magnetization direction (fig.6).

For a clear identification of TAMR we have performed magnetoresistance scans with different directions of the magnetic field in the plane. In these scans, the coercive fields of the two switching events (H_{C1} and H_{C2}) vary depending on the relative orientation of the magnetic field with respect to the easy axes. Experimental data obtained on our type-3 sample are shown in fig. 5 (0° and 90° are the two sample diagonals, see also Fig.1).

The effect is even clearer in a magnetoresistance plot where the two scans for field orientations of 0° and 90° are shown together on the same scale (fig. 6). For 90° the resistance is in the high-state in magnetic saturation[13], and it is low between H_{C1} and H_{C2} , while for 0° orientation the resistance in saturation is in its low-state and it is high in between H_{C1} and H_{C2} . These two directions are the main axes which determine the minimum and maximum value of the tunneling resistance. The observation that the maximum resistance value between H_{C1} and H_{C2} (0° curve) is higher than the maximum resistance in saturation (90° curve) can be explained by the occurrence of multi-domain behavior in which parts of the sample are magnetized out of plane due to a weak out-of-plane easy axis. Supporting SQUID measurements (fig. 7) indeed show a remanent magnetization component perpendicular to the surface.

Still further information comes from a magnetoresistance scan on the type-3 sample in which the direction of the B-field is rotated by 360° in the plane while its magnitude is kept constant close to saturation (full saturation is not possible in our magnet). For ordinary TMR with two ferromagnetic electrodes this scan must always show the same resistance value because the two layers are always aligned in parallel. For our sample we see an anisotropic resistance distribution (fig. 8), clearly indicating the presence of TAMR.

In an additional control experiment, we also measure the intrinsic magnetoresistance of the LSMO layer in order to exclude any contribution from the bulk. The signal is of the order of a few Ω and shows no switching events. This bulk magnetoresistance is too small to be resolved on the scale of the total signal of a type-3 stack.

We have thus demonstrated that TAMR can exist in OSV structures with at least one LSMO electrode. This effect opens up new perspective for organic spintronics. However, as the effect can be either positive or negative in sign, depending on the direction of the

applied magnetic field, our observations imply that careful measurements on any OSV are necessary in order to distinguish between TAMR and real spin valve operation. Moreover, the observation of TAMR in the type-3 devices indicates, that even for OSC layers of more than 100 nm thickness, tunneling effects at the interfaces can be the dominating transport mechanism.

We thank the EU for funding the research in the project OFSPIN.

-
- [1] V. Dediu *et al.*, Solid State Commun. **122**, 181-184 (2002).
 - [2] Z. H. Xiong, D. Wu, Z.V. Vardeny, and J. Shi, Nature **427**, 821-824 (2004).
 - [3] S. Majumdar, H.S. Majumdar, R. Laiho, and R. sterbacka, J. Alloys Compd. **423**, 169-171 (2006).
 - [4] W. Xu *et al.*, Appl. Phys. Lett. **90**, 072506 (2007).
 - [5] F.J. Wang *et al.*, Synth. Met. **155**, 172-175 (2005).
 - [6] T.S. Santos *et al.*, Phys. Rev. Lett. **98**, 016601 (2007).
 - [7] J.H. Oh *et al.*, Appl. Phys. Lett. **91**, 212107 (2007).
 - [8] C. Gould *et al.*, Phys. Rev. Lett. **93**, 117203 (2004).
 - [9] C. Rüster *et al.*, Phys. Rev. Lett. **94**, 027203 (2005).
 - [10] K. I. Bolotin, F. Kuemmeth, and D.C. Ralph, Phys. Rev. Lett. **97**, 127202 (2006).
 - [11] J. Moser *et al.*, Phys. Rev. Lett. **99**, 056601 (2007).
 - [12] B.G. Park *et al.*, Phys. Rev. Lett. **100**, 087204 (2008).
 - [13] By saturation, we mean a field large enough to perfectly align the magnetization to the direction of the external field.
 - [14] T.L. Francis, Ö Mermer, G. Veeraraghavan, and M. Wohlgenannt, New J. Phys. **6**, 185 (2004).
 - [15] M.A. Baldo and S.R. Forrest, Phys. Rev. B **64**, 085201 (2001).
 - [16] R.P. Cowburn *et al.*, J. Appl. Phys. **78**, 7210 (1995).

FIG. 1: Schematic drawing of the vertical transport structure (a). A is the bottom contact material and B is the top contact material as listed in table 1 for the respective samples. (b) Structure of the PTCDI-C4F7 molecule (b)

FIG. 2: Magnetoresistance trace of a PTCDI-C4F7-based vertical OSV structure with an LSMO bottom electrode and a CoFe top electrode (type-1 sample). A 30% spin-valve effect is superimposed to a background signal. The LSMO layer switches its magnetization state at 3 mT while the CoFe contacts have a coercive field of approx. 100 mT.

FIG. 3: Magnetoresistance trace of a PTCDI-C4F7-based vertical transport structure with only Al-electrodes. No magnetoresistance can be detected.

FIG. 4: I/V characteristics of the layer stack with LSMO bottom electrode and aluminum top electrode (type-3 sample). The I/V characteristics are symmetric and from room temperature to 4.2 K the resistance increases by approx. one order of magnitude.

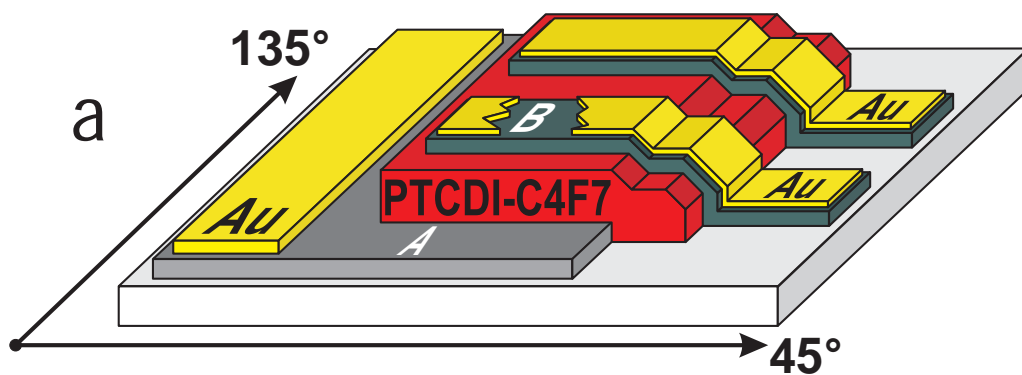
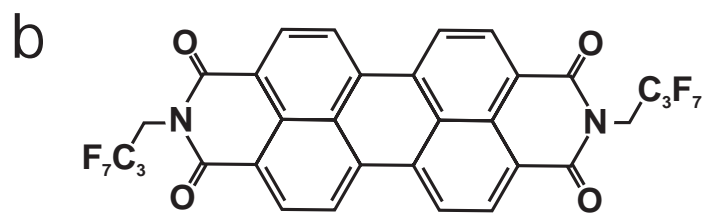
FIG. 5: Magnetoresistance sweeps for the TAMR test sample with the magnetic field applied in different directions in the plane. After each scan the field direction is rotated by 30° . 0° and 90° are the sample diagonals. For 90° and 270° the switching event is towards negative values. For clarity, scans for different directions are offset by $850 \text{ k}\Omega$

FIG. 6: Magnetoresistance traces (type-3 sample) with the magnetic field aligned along 0° and 90° . At large positive or negative fields two different resistance states can be distinguished, a clear signature of TAMR. For the scan in 0° direction, the spin-valve signal is positive while it is negative for the 90° sweep.

FIG. 7: Magnetization curve of the LSMO layer with the external field applied perpendicular to the surface. Between -50 mT and $+50 \text{ mT}$ (insert) a remanent magnetization is observed, indicating some out of plane anisotropy component. At 1 T the magnetization is saturated perpendicular to the sample surface. The signal at higher fields is caused by a paramagnetic contribution of the substrate.

FIG. 8: Magnetoresistance scan (type-3 sample) taken at constant field while the angle of the applied field is slowly rotated by 360° . The scan clearly shows the minimum and maximum resistance state at $\Phi=0^\circ/180^\circ$ and $\Phi=90^\circ/270^\circ$, respectively, corresponding to the saturation states in Fig. 6.

Fig1 Gruenewald et al.



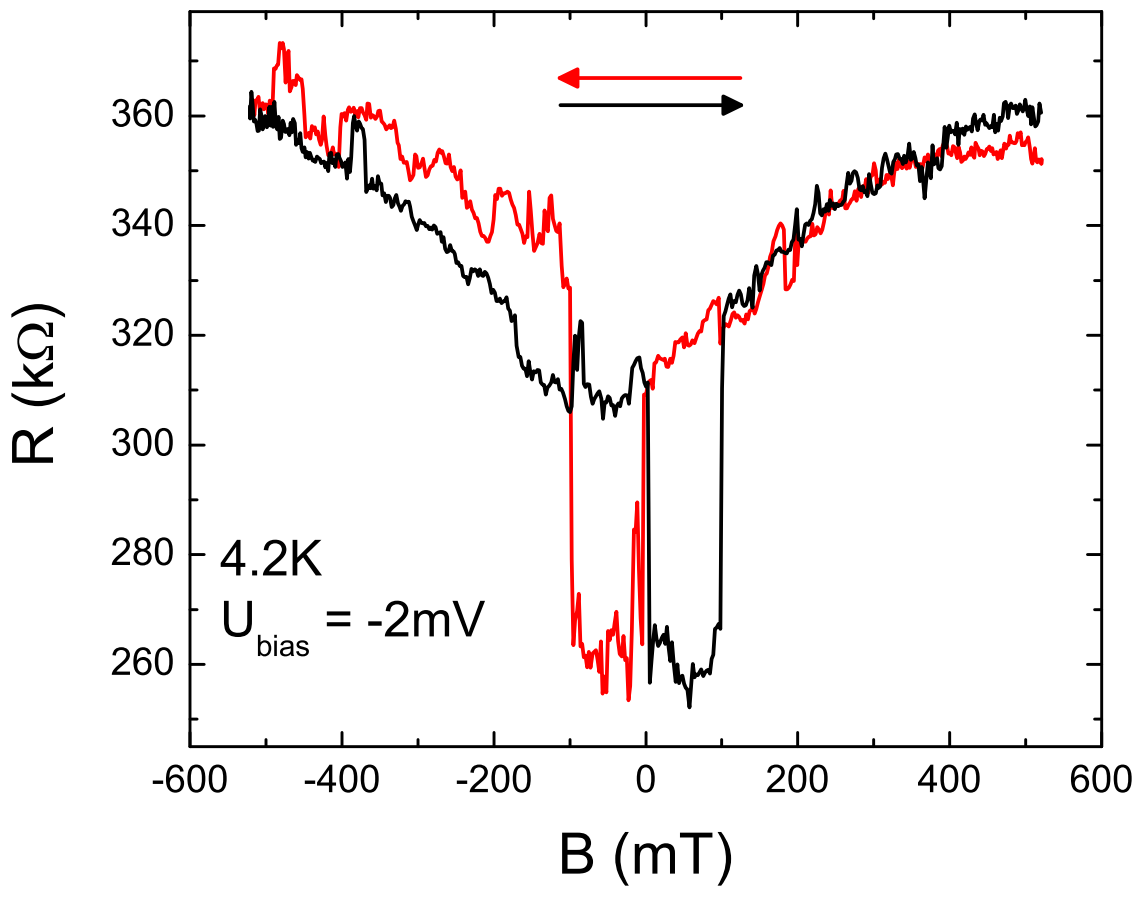


Fig2 Gruenewald et al.

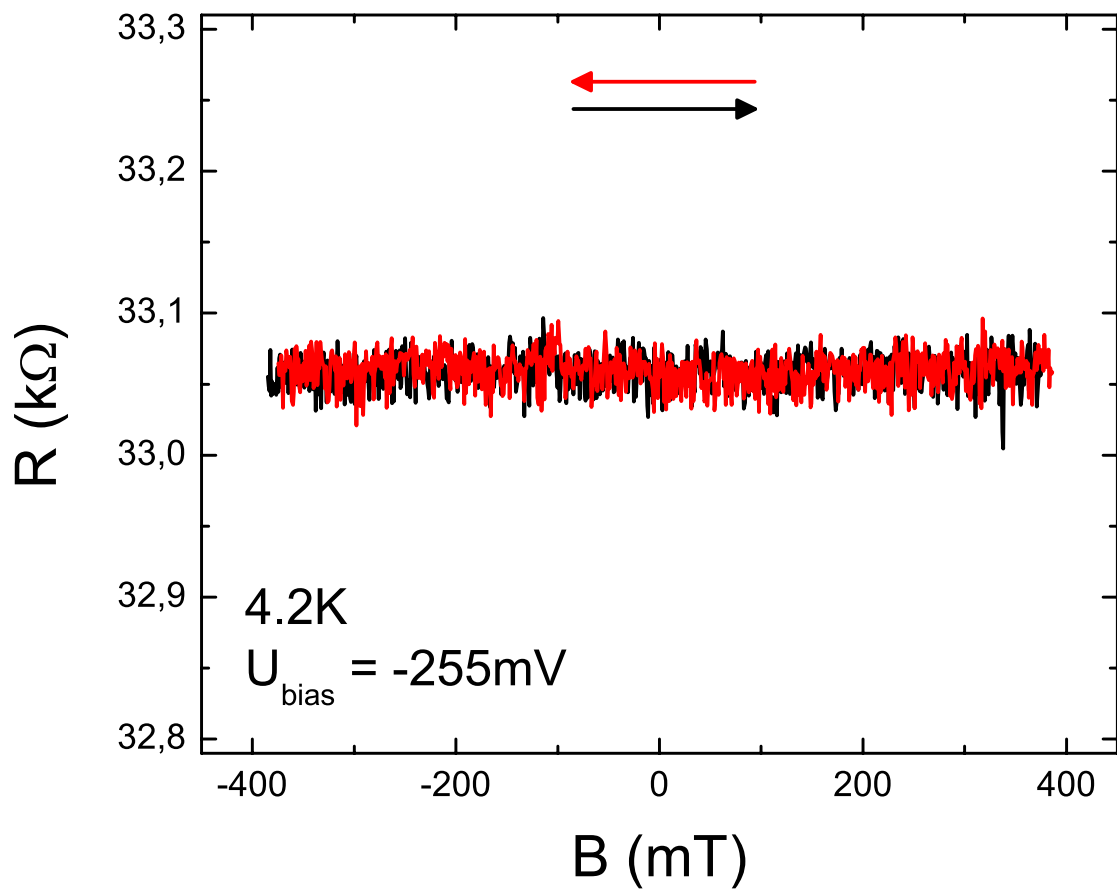


Fig3 Gruenewald et al.

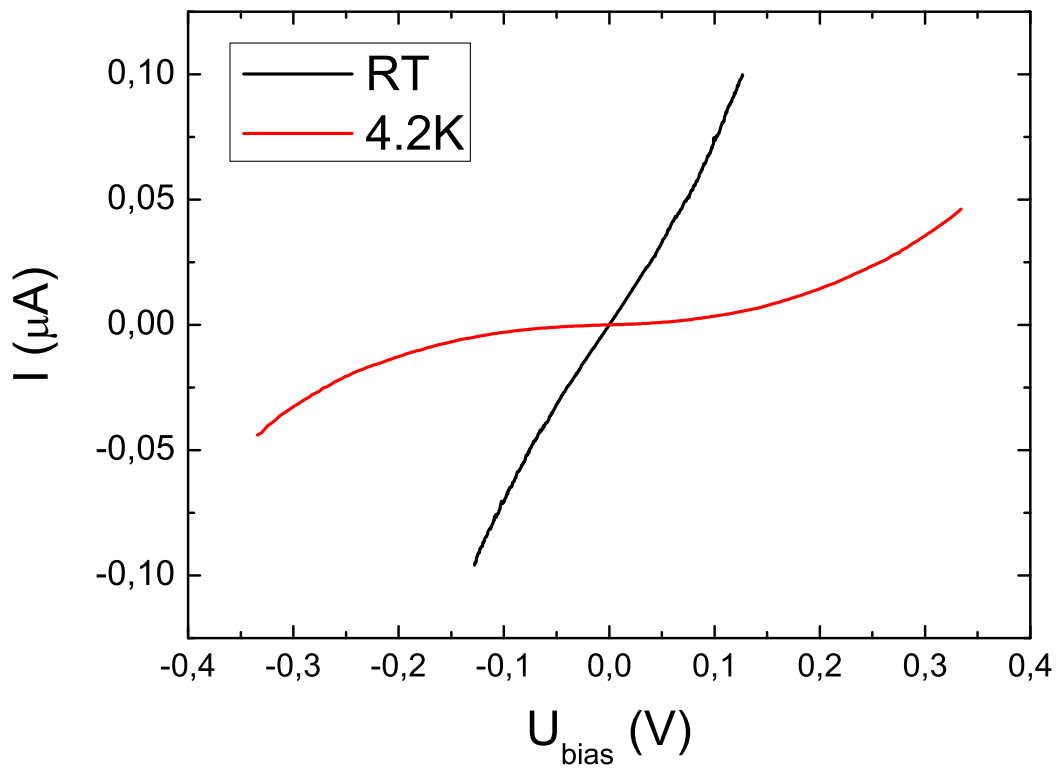


Fig4 Gruenewald et al.

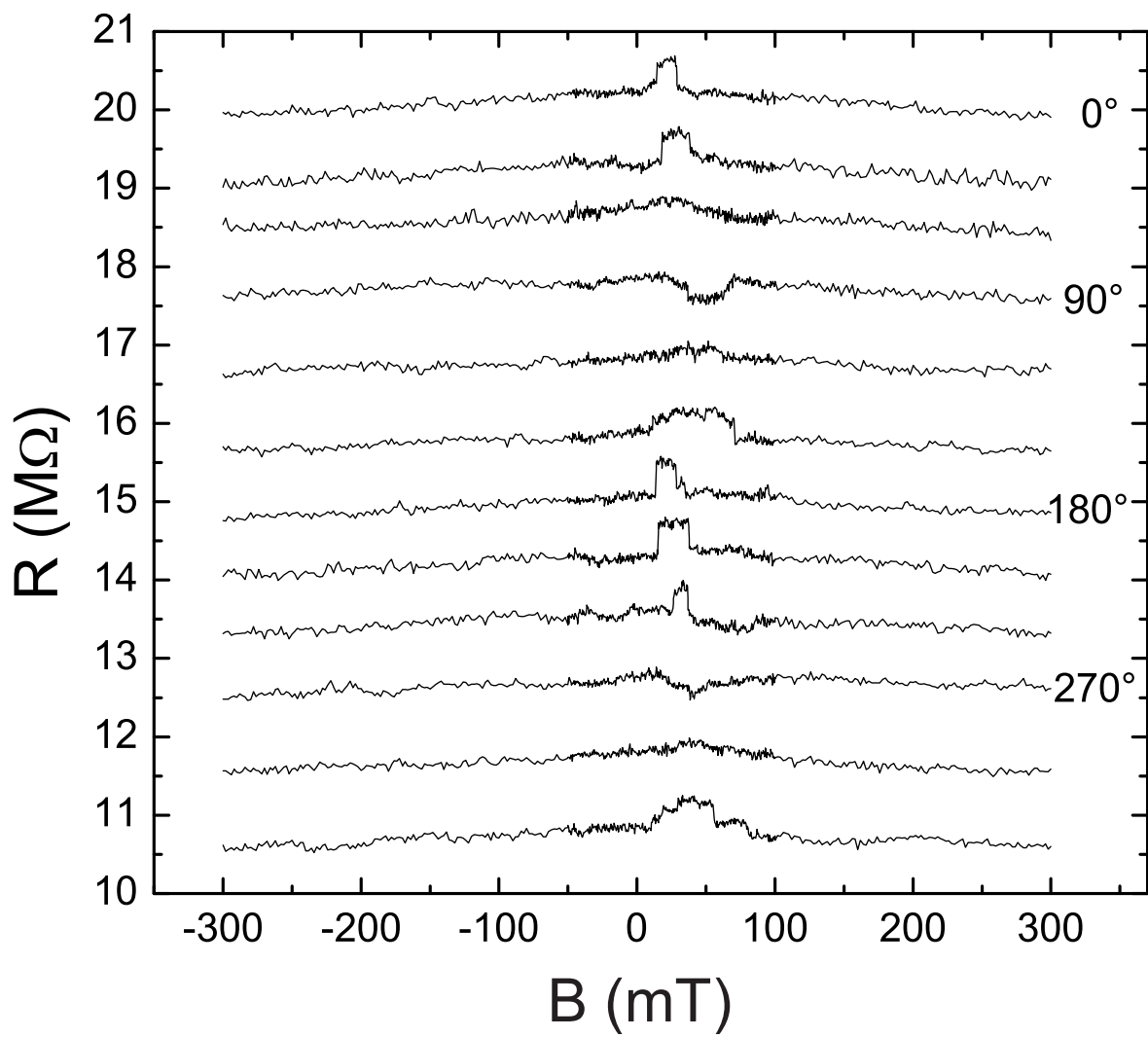


Fig5 Gruenewald et al.

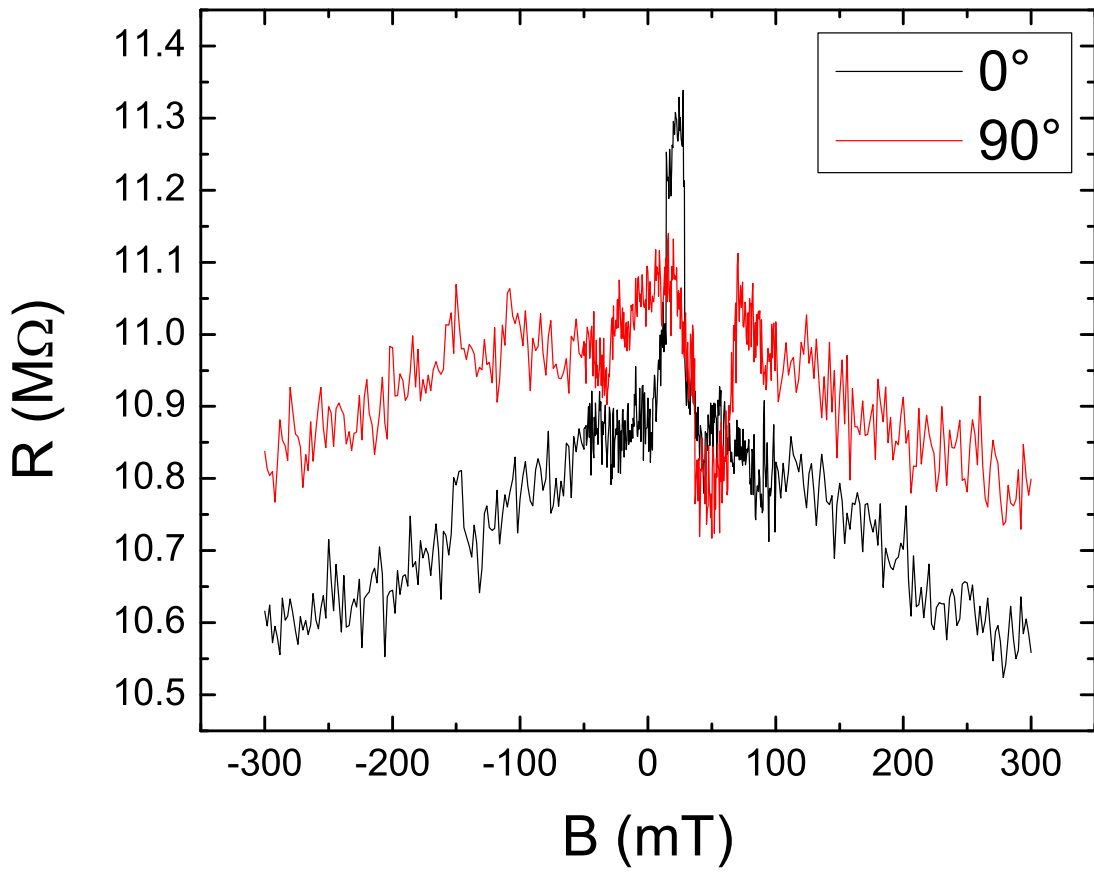
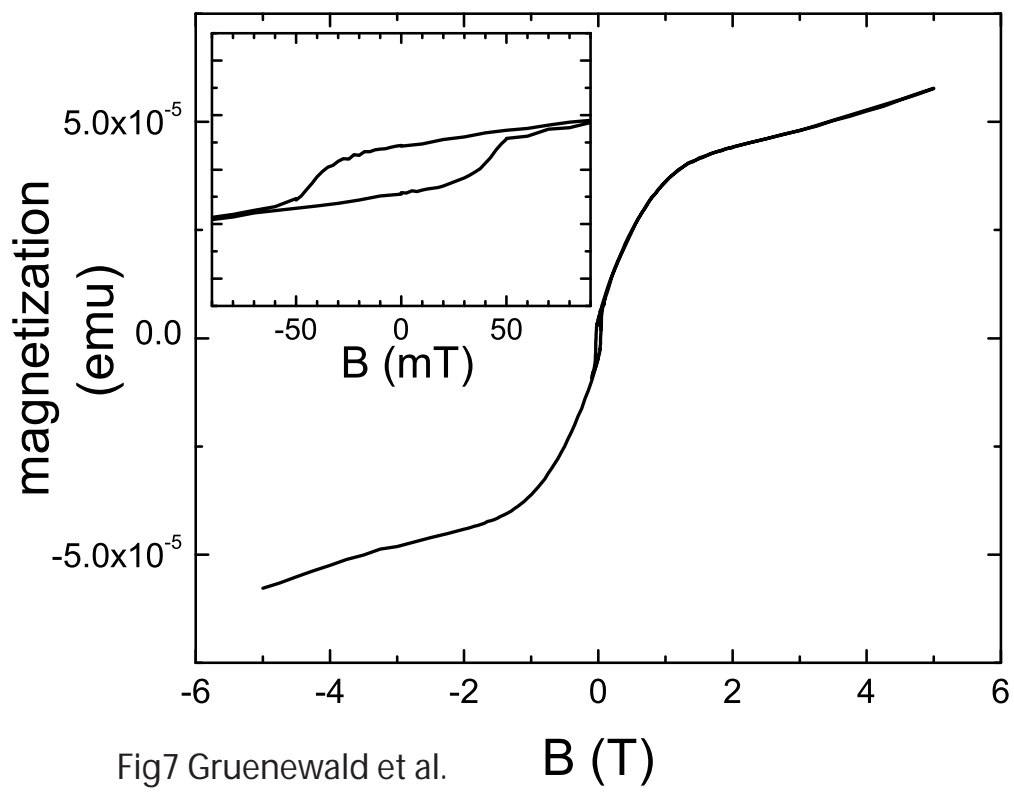


Fig6 Gruenewald et al.



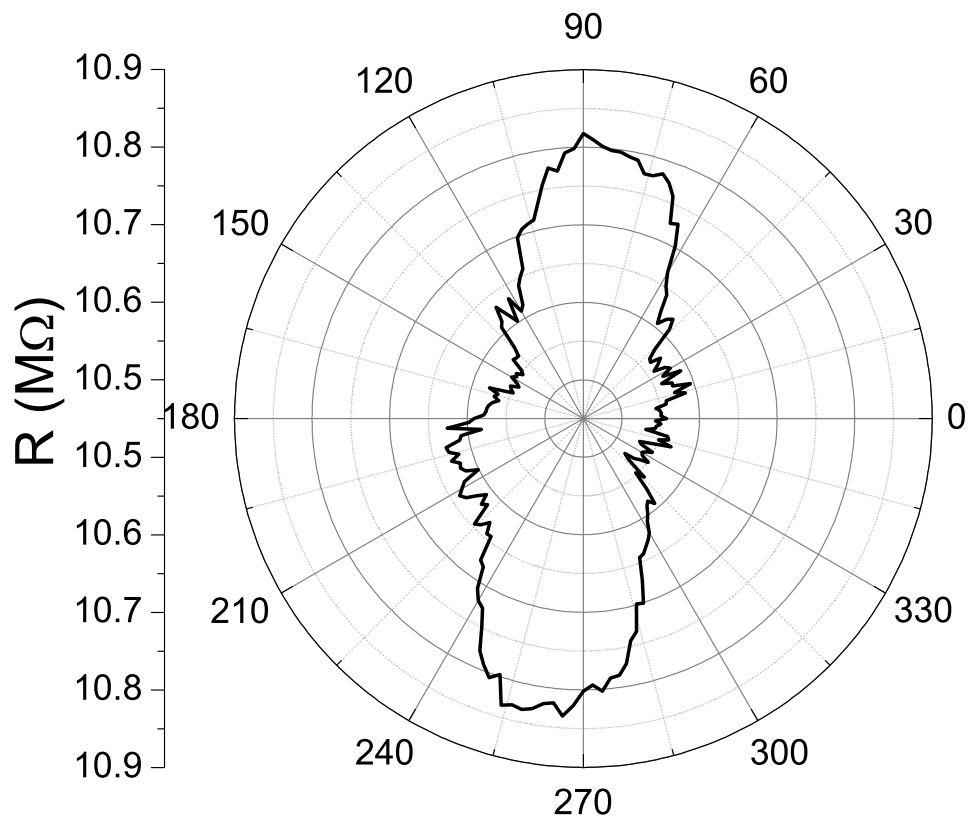


Fig8 Gruenewald et al.